



Published in final edited form as:

Med Sci Sports Exerc. 2018 May ; 50(5): 945–956. doi:10.1249/MSS.0000000000001519.

Beneficial Effects of Exercise Pretreatment in a Sporadic Alzheimer's Rat Model

Chongyun Wu^{1,a}, Luodan Yang^{2,a}, Donovan Tucker², Yan Dong², Ling Zhu¹, Rui Duan¹, Timon Cheng-Yi Liu¹, and Quanguang Zhang^{1,2}

¹Laboratory of Laser Sports Medicine, College of Physical Education and Sports Science, South China Normal University, University Town, Guangzhou, China

²Department of Neuroscience and Regenerative Medicine, Medical College of Georgia, Augusta University, Augusta, GA

Abstract

PURPOSE—This study aimed to examine the effects of swimming exercise pretreatment on a streptozotocin (STZ)-induced sporadic Alzheimer's disease rat model and provide an initial understanding of related molecular mechanisms.

METHODS—Male 2.5-month-old Sprague-Dawley rats were divided into the following 4 groups: a) control, b) swim + vehicle, c) STZ without swim, and d) swim + STZ. The Barnes Maze task and Novel Object Recognition test were used to measure hippocampus-dependent spatial learning and working memory, respectively. Immunofluorescence staining, Western blot analysis, ELISA analysis and related assay kits were used to assess synaptic proteins, inflammatory cytokines, total antioxidant capacity, antioxidant enzymes, amyloid-beta (A β) production and tau hyperphosphorylation.

RESULTS—Behavioral tests revealed that exercise pretreatment could significantly inhibit STZ-induced cognitive dysfunction ($p < 0.05$). STZ animals displayed significant loss of pre/post-synaptic markers in the hippocampal CA1 that was reversed by exercise pretreatment ($p < 0.05$). STZ rats also displayed increased reactive gliosis, release of pro-inflammatory cytokines, and oxidative damage, effects attenuated by pre-exercise ($p < 0.05$ between-treatment changes). Likewise, pre-exercise significantly induced protein expression ($p < 0.001$) and DNA-binding activity ($p = 0.015$) of Nrf2 and downstream antioxidant gene expression in the hippocampal CA1 region ($p < 0.05$). STZ rats had increased levels of A β (1-42) and tau hyperphosphorylation that were significantly ameliorated by exercise ($p < 0.05$). Histological studies showed exercise imparted substantial neuroprotection ($p < 0.001$), suppressing neuronal apoptosis-like cell death in the hippocampal CA1 compared to STZ control group ($p < 0.001$).

Corresponding author: Quanguang Zhang, Ph.D., qzhang@augusta.edu, Department of Neuroscience and Regenerative Medicine, Medical College of Georgia, Augusta University, 1120 15th Street, Augusta, GA.

^aChongyun Wu and Luodan Yang contributed equally to this work.

Statement of interest

The authors declare that there is no conflict of interest in the current study.

The results of the study are presented clearly, honestly, and without fabrication, or inappropriate data manipulation.

The results of the present study do not constitute endorsement by ACSM.

CONCLUSION—Exercise pre-training exerts multifactorial benefits on AD that support its use as a promising new therapeutic option for prevention of neurodegeneration in the elderly and/or AD population.

Keywords

Pre-exercise; Cognition improvement; Inflammation; Oxidative stress; Neuroprotection

Introduction

Alzheimer's disease (AD) is a progressive neurodegenerative disorder and is the most common form of dementia, resulting in irreversible cognitive deficits and impaired learning ability (1). AD exacts a heavy medical, financial, and emotional burden, robbing both patients and families of quality of life. This is compounded by a lack of adequate therapeutic options to slow or halt the inexorable advance of the disease. AD pathology is classically characterized by amyloid-beta ($A\beta$) protein aggregates, otherwise known as senile plaques (SP), and intracellular neurofibrillary tangles (NFT) comprised of hyperphosphorylated tau (1). AD is also accompanied by neuroinflammation, reactive gliosis, oxidative stress, and neuronal loss. There has recently been extensive research interest in discovering non-pharmacological interventions to treat or perhaps cure AD. Within this surge of interest, the therapeutic effects of exercise have garnered significant attention (1, 2). Multiple studies have indicated that exercise training after the development of AD can exert neuroprotection by decreasing $A\beta$ deposition, ameliorating inflammation, enhancing synaptic plasticity, and inhibiting neuronal apoptosis (1–3). The beneficial effects of exercise in the context of AD have investigated in several additional studies as well, with promising results (4–7).

Oxidative stress, exacerbated by the process of aging, is an early pathological feature of AD and is widely accepted to play a key role in the progression of the disease (8). Reactive oxygen species (ROS) react with cellular lipids, proteins, and DNA/RNA to generate damaging lipid peroxides, protein carbonyls, and DNA/RNA modifications, respectively. As well, oxidative stress contributes to $A\beta$ generation and NFT formation (8). One study has demonstrated that the nuclear erythroid 2-related factor 2/ antioxidant response element (Nrf2/ARE) pathway plays an important role in neuroprotection by responding to oxidative stress in the brain, and this protective role is compromised in the AD brain (9).

$A\beta$ deposition induces an inflammatory response that contributes to a dangerous feedback cycle that advances progression of the disorder (10). This inflammatory response is driven by glial activation. In healthy conditions, microglia and astrocytes protect the brain against pathogens and contribute to the ongoing maintenance homeostasis of brain tissue (11, 12). In the AD brain, however, microglia and astrocytes activate and surround SP (11). Upon activation, glial cells begin to release pro-inflammatory mediators including TNF- α , IL-1 α , IL-1 β , IL-6, IL-18 and IL-23 which induce neighboring cells to activate, stimulating them to activate and secrete more pro-inflammatory factors, perpetuating inflammation in a feed-forward manner (11). Microglia respond to activation in the AD brain by decreasing secretion of anti-inflammatory cytokines (IL-4, IL-10), further contributing to a pro-

inflammatory, detrimental neuronal microenvironment that accelerates neurodegeneration and hampers neuronal repair (1).

Synaptic loss is widely regarded as a hallmark of AD, with AD patients presenting significant loss of hippocampal neurons post-mortem (13). In recent years, growing evidence suggests that synaptic loss occurs prior to other pathological components of AD, and that this process is closely linked to cognitive impairment (14). In fact, some studies suggest that synapse loss is a more accurate indicator of cognitive impairment than other biomarkers of AD progression (14). Pre-synaptic and post-synaptic proteins, such as synaptophysin and spinophilin, respectively, are commonly used as markers of synaptic changes, and their expression is decreased in AD (15, 16). As cognitive decline is the most apparent and distressing symptom affecting AD patients, synaptic loss and treatments that can prevent it are of critical importance.

In recent years, researchers have examined the effect of exercise based therapies for AD treatment (1, 2). Accumulating evidence demonstrates that exercise can decrease A β deposition, chronic inflammation, restore cognitive function, and potentially improve quality of life for those suffering from AD (1, 2). Our previous study indicated that treadmill exercise after AD development conferred neuroprotection by regulating the polarization of microglia and attenuating streptozotocin (STZ)-induced oxidative stress. In addition, we demonstrated that 4 weeks of treadmill training reduced the accumulation of A β and tau hyperphosphorylation (1). While many studies, including our own, have investigated the neuroprotective role of exercise training, these studies were primarily concerned with the alleviating effects of exercise after the AD model was established, rather than investigating the potential preventative role of exercise prior to AD pathology.

Therefore, the current study was designed to examine the preventive effect of 4 weeks of swimming exercise pre-training on inhibiting synaptic and neuronal loss, ameliorating inflammation, and reducing oxidative stress in a sporadic AD rat model. These effects were in tandem with impressive neuroprotection that bodes well for exercise a potent preventative measure for AD.

Materials and Methods

Animals

Young adult male Sprague Dawley rats (2.5 months old, Charles River Laboratories, Charleston, SC, USA) were used in this study. Rats used in this project were maintained in propylene cages in an environment with ambient temperature of 22–24 °C with humidity kept between 50–60%. Rats were randomly separated into four groups (n = 8–10 in each group): a) control (no swim and vehicle injection, Cont), b) swim + vehicle injection (SW + Veh), c) STZ injection with no exercise (STZ), and d) swim + STZ injection (SW + STZ). All animals were allowed ad libitum access to water and food and were maintained on a 12/12 light-dark cycle. All procedures were approved by our Institutional Animal Care and Use Committee.

Exercise Pretreatment Protocol

Exercise training was performed in barrels (55 cm in diameter; 60 cm in height) for 4 weeks in 35 ± 1 °C water. In the process of swimming exercise, rats were prevented from floating motionlessly via light agitation. The schematic diagram of the study is presented in Fig 1. For exercise pretreatment groups, in the first two days, the training began with 10 min/day, and was increased by 10 min every two days until duration reached 1 h/day, occurring at day 12. After this point, training was maintained at 1 h/day until day 26. STZ injections were performed on day 29, and behavioral testing began 3 weeks later. Rats were sacrificed on day 56 and brains were extracted for further analysis.

STZ Model

ICV injection of STZ was performed as described in our previous study (1). In brief, STZ was administered via ICV injection with STZ (30 µg/µl) under anesthesia (sodium pentobarbital, 50 mg/kg, i.p.) in a stereotaxic frame. A Hamilton microsyringe was used to inject STZ at a rate of 0.5 µl/min with a total STZ delivery of 2.4 mg/kg. The injection coordinates relative to bregma were set as follows: posterior: -0.8 mm, lateral: ± 1.5 mm, depth: -3.5 mm. Identical procedures were conducted in the control group with saline rather than STZ. Rectal temperature was maintained at 36.5 to 37.5 °C throughout the experimental procedures using a heating pad.

Brain Preparation and Histological Analysis

As our previous study described (1), rats were sacrificed, after behavioral tests, under deep anesthesia with sodium pentobarbital followed by transcardial perfusion with 0.9% ice-cold saline. The rats were decapitated and their brains were removed and postfixed with 4% paraformaldehyde (PFA) at 4°C overnight, then transferred to 30% sucrose for cryoprotection until they sank. Brains were immersed in OCT cryoprotectant and frozen 80 °C overnight. Coronal brain sections (20 µm) were prepared with a Leica Cryostat (Leica Biosystems; Buffalo Grove, IL, USA). For cresyl violet staining, brain sections were selected and stained by 0.01% (w/v) cresyl violet for 10 min after graded ethanol dehydration. TUNEL staining was carried out using Click-iT Plus TUNEL assay kit (Thermo Scientific; Rockford, IL, USA) according to the manufacturer's instructions. Stained sections were imaged by LSM510 Meta confocal laser microscope (Carl Zeiss; Thornwood, NY, USA). Histological counting analysis of the staining was carried out using the methods as described previously by our laboratory (1). Briefly, 3–5 representative sections in the coronal plane of the dorsal hippocampus (at least 200 micron apart, ~2.5–4.5 mm posterior from Bregma) of each animal were selected for analysis. The intact, normal-appearing cells in the hippocampal CA1 pyramidal layer, displaying round soma and pale stained nuclei as in normal control animals, were counted as surviving neurons. The CA1 cells with abnormal-appearing pyknotic, condensed and shrunken nuclei were considered to be nonviable neurons. The numbers of surviving neurons and TUNEL-positive cells were counted per 250 µm length of medial hippocampal CA1 region on every sample from both the left and right hemispheres, and the single value of the cell counts for each animal were calculated from the averaged value from both hippocampi on each of the examined sections. Cell counting was performed by investigators blinded to the histological staining on a light

microscope. Data were expressed as mean \pm standard error (SE) from five to eight ($n = 5-8$) independent animals in each group.

Immunofluorescence Staining

Immunofluorescence staining was performed as in our previous study (1). Briefly, floating coronal brain sections (20 μm) were first blocked by 10% normal donkey serum in PBS for 1 h at room temperature, followed by incubation with primary antibodies overnight at 4°C in PBS containing 0.4% Triton X-100. The primary antibodies used in present study are as follows: anti-synaptophysin and spinophilin (1:100, Abcam; Cambridge, MA, USA); anti-Iba1 (1:1000), GFAP (1:500), IL-10 (1:50), Nrf2 (1:50), TRX2 (1:50), NQO-1(1:50) and PARP1 (1:50) (Proteintech Group; Rosemont, IL, USA); anti-malondialdehyde (MDA) (1:100, Novus Biologicals; Littleton, CO, USA). After incubation with primary antibodies for 48 h, the brain sections were then washed with PBS/0.4% Triton 3 times for 30 min each, followed by incubation with matching Alexa Fluor donkey anti-mouse/rabbit/goat second antibodies (594/647/488, Thermo Fisher) for 1 h in the dark. Thereafter, sections were mounted with DAPI Fluoromount-G (SouthernBiotech; Birmingham, AL, USA) or Vectashield mounting medium (H-1200, Vector Laboratories; Burlingame, CA, USA). Images were captured using an LSM510 Meta confocal laser microscope (Carl Zeiss; Thornwood, NY, USA), and quantitatively analyzed using ImageJ software (Version 1.49; NIH; Bethesda, Maryland, USA).

Brain Homogenates

Brain homogenization and western blot analyses were carried as our previous study described (1). In brief, tissues were homogenized using a motor-driven Teflon homogenizer in ice-cold buffer A containing 50-mM 4-(2-hydroxyethyl)-1-piperazineethanesulfonic acid [HEPES], pH 7.4, 150-mM NaCl, 12-mM β -glycerophosphate, 1% Triton X-100, 3 mM dithiothreitol (DTT), 2 mM sodium orthovanadate (Na_3VO_4), 1 mM EGTA, 1 mM NaF, 1mM phenylmethylsulfonyl fluoride (PMSF), and inhibitors of proteases and enzymes (Thermo Scientific; Rockford, IL, USA). Then, the homogenates in tubes were vigorously mixed for 20 min and centrifuged at 15,000 $\times g$ for 30 min at 4°C, and total protein fractions in the supernatants were collected and stored for use. For the extraction of cytosol fractions and nuclear fractions, tissues were homogenized in ice-cold buffer containing 10-mM HEPES (PH 7.9), 1-mM DTT, 1-mM Na_3VO_4 , 1,4-nitrophenyl phosphate (PNPP), and inhibitors of proteases and enzymes. After swelling on ice for 10 min, the homogenates in tubes were vigorously mixed for 30 s and centrifuged at 800 g for 10 min after the addition of NP-40 (0.6% of total solution) to get supernatants. Then the supernatants were centrifuged at 15,000 $\times g$ for 30 min at 4 °C to get cytosolic fractions in the supernatants. The resulting nuclear pellets were washed three times using buffer A and resuspended in buffer B containing 20-mM HEPES (PH 7.9), 400-mM NaCl, 20% glycerine, 1-mM DTT, 1-mM Na_3VO_4 , 1-mM PNPP, and inhibitors of proteases and enzymes. After rocking at 4 °C for 30 min, the remaining homogenates were centrifuged at 12,000 $\times g$ for 20 min to get nuclear fractions. The concentration of total protein was determined by Modified Lowry Protein Assay (Pierce; Rockford, IL, USA).

Western Blot Analysis

For western blot analysis, protein of each sample (50 µg) were separated by electrophoresis apparatus (Bio-Rad; Hercules, CA, USA) with 4–20 % sodium dodecyl sulfate-polyacrylamide, and transferred to PVDF membrane. The PVDF membranes were then blocked, followed by incubation overnight at 4 °C with the following primary antibodies: anti-HO-1 (1:200) and SOD2 (1:500) (Proteintech Group, Rosemont, IL, USA), anti-PHF1 (1:500, Thermo Scientific; Rockford, IL, USA). After 3 washes (15 min each), the membrane was incubated with HRP-conjugated secondary antibodies (1:1000, Cell Signaling; Danvers, MA, USA) for 1 h at room temperature. The images of bound proteins were captured by CCD digital imaging system, and the ImageJ software were used to analyze the bands. For analyses of the band densities, band densities for the indicated proteins were normalized to housekeeping protein (GAPDH).

Inflammatory Cytokines Assay

ELISA analysis was used to determine the levels of pro-inflammatory and anti-inflammatory cytokines in brain homogenates. Briefly, protein samples of different groups containing the same amount of proteins were diluted in carbonate coating buffer (Sigma-Aldrich; St. Louis, MO, USA) to 50 µL. Samples (50 µL) were loaded in PVC ELISA microplate (Corning, New York, NY, USA), then sealed and incubated overnight at 4 °C. After discarding the samples, the remaining protein-binding sites were blocked by blocking buffer (1% BSA in PBS, 0.3% solution of H₂O₂) for 1 h at room temperature. Samples loaded in wells were incubated with 50 µL primary antibodies overnight at 4 °C followed by incubation with HRP conjugated secondary antibodies for 1 h at room temperature. Following three washes, the plates were incubated with TMB (3, 3', 5, 5' -tetramethylbenzidine, BD Biosciences; San Jose, CA, USA) substrate reagent for 30 min. Subsequently, 50 µL of sulfuric acid was administered to stop the reaction and the plate was read at 450 nm on a spectrophotometer (Bio-Rad; Hercules, CA, USA). The minimal and maximal absorbance of the low and high standards was in the range of 0.10 to 1.50, and the absorbance values of the samples range from 0.30 to 0.99. The coefficient of variation between all duplicates was lower than 15%.

Nrf2 DNA-binding Activity Assay

Nrf2 transcription factor assay kit (600590; Cayman Chemical; Ann Arbor, MI, USA) was used to measure the level of Nrf2 DNA-binding activity. In brief, the aforementioned nuclear extract (10 µl) was mixed with 90 µl of Complete Transcription Factor Binding Assay Buffer (CTFB) followed by incubation for 1 h at room temperature. In positive or blank control wells, 10 µl of the provided nuclear extract or CTFB was added instead of the samples. After discarding the samples and washing the plate five times, the samples loaded on the wall were incubated with 100 µl of diluted Nrf2 antibody at room temperature for 1 h followed by HRP conjugated secondary antibodies incubation for another 1 h at room temperature. Following five washes with wash buffer, the plate was incubated with transcription factor developing solution (100 µl) until the blue color turned medium to dark blue and then stop solution was added and absorbance was read on a spectrophotometer at 450 nm. Nrf2 DNA-binding activity was calculated and expressed as percentage changes versus control group.

Total Antioxidant Capacity

Total antioxidant capacity was measured by an antioxidant assay kit (709001; Cayman Chemical; Ann Arbor, MI, USA) according to the instructions of the vendor. The principle of this assay is that antioxidants in the sample could prevent ABTS (2,2'-Azino-di-[3-ethylbenzthiazoline sulphonate]) oxidation, and the capacity of the sample to do so could be expressed after comparison with that of trolox. Briefly, samples (10 μ L) prediluted in assay buffer were added to the designated wells with 10 μ L of metmyoglobin and 150 μ L of chromogen. After adding 40 μ L of hydrogen peroxide working solution to the designated wells, the plates were sealed and incubated for 5 min on a shaker. Thereafter, absorbance at 750 nm was recorded on a spectrophotometer and the standard was plotted as a function of the final trolox concentration (mM) according to the assay protocol. Antioxidant capacity of each sample was then determined using the trolox standard curve, and the values were reported as percentage changes compared to the control group.

Protein Carbonyl Determination

To measure the level of protein carbonyls, the OxyBlot Protein Oxidation Detection Kit (S7150; EMD Millipore; Burlington, MA, USA) was used. Briefly, proteins of each sample (20 μ g) were denatured by adding 5 μ L of 12% SDS for a final concentration of 6% SDS. Then 10 μ L of 1X DNPH Solution were added to derivatize the samples. After incubation at room temperature for 15 min, samples were mixed with 7.5 μ L of neutralization solution. Then samples were loaded in PVC ELISA microtiter plate, and the levels of protein carbonyl were measured by ELISA analysis.

Measurement of A β (1–42) Levels

The levels of A β were measured by using A β (1–42) immunoassay Kit (KMB3441; Thermo Scientific; Rockford, IL, USA) as described in our previous study (1). Detergent-soluble A β (1–42) levels were measured in protein samples collected as described above. Briefly, equal amounts of protein in each group were diluted to 100 μ L and incubated in plate wells for 2 h at room temperature. Plate wells were then washed and incubated with the Detection Antibody solution followed by washes and incubation with HRP-linked antibody solution in accordance with the manufacturer's instruction. Finally, absorbance was read at 450 nm on a spectrophotometer (Bio-Rad; Hercules, CA, USA) after the adding of Stop Solution. A β levels were calculated and expressed as percent changes versus control group.

Barnes Maze

The Barnes maze task, a widely accepted behavior test to evaluate hippocampus-dependent spatial learning in rodents, was performed as described previously by our laboratory (1). A 100 cm high circular platform with a diameter of 122 cm was used. There are 18 holes located around the perimeter with a black escape box (20 \times 15 \times 12 cm) placed under one of these. Surrounding the table are four dividers with distinct shapes attached to facilitate place learning. The task was divided into 2 stages: stage 1, training trials on day 50, 51 and 52; and stage 2, and a probe test on day 53. During training trials, the animal is placed on the table and given 3 min to find and enter the escape box, with bright lights and a metronome serving as aversive stimuli. Each animal performed 1 trial per day during the training stage.

On the probe test day, the black escape box was removed and the time spent in the quadrant where the escape box was originally located was recorded by an overhead video camera and analyzed with ANY-maze video tracking software (Stoelting; Wood Dale, IL, USA). After each test, the platform was cleaned with 70% ethanol and dried with a blower fan. Time spent in the target area was quantified and analyzed after the test.

Object Novel Object Recognition (NOR)

The NOR test was performed to test recognition memory, a hippocampus-dependent working memory (1). An empty box (40 × 50 × 50 cm) was used in this task. In the first day, the rats were allowed to explore freely in the empty box for 5 min. On the second day, two identical objects were fixed to the floor at an equal distance and the rats were also given 5 min to explore. On the third day (choice day), an object was changed to a novel object, and the rats were then returned to testing field. The time spent on exploring an old or new object was recorded for 5 min by ANY-maze video tracking software. Exploration of an object was defined as the animal's nose being in the zone at a distance of 2 cm.

Statistical Analysis

Statistical analyses were performed using SigmaStat software (Systat Software; San Jose, CA, USA) and ANY-maze software (Stoelting; Wood Dale, IL, USA) when applicable. All dependent variables were analyzed between groups using one-way analysis of variances (ANOVAs) with Student-Newman-Keuls (S-N-K) post hoc tests. All dependent variables with multiple time point measures were analyzed using two-way (group*time) repeated measures of ANOVAs. In the event that a significant group*time interaction occurred, S-N-K post hoc tests were performed between groups at each time point, and within-group dependent samples *t*-tests were performed to detect significant pre-to-post changes within each treatment. All data were presented as the mean ± SE. A value of $P < 0.05$ was considered significant for all statistical tests.

Results

Exercise Pretreatment Significantly Ameliorates STZ-induced Learning and Memory Deficits in Barnes Maze Task and Novel Object Recognition Test

The Barnes Maze Task was performed to assess hippocampus-dependent spatial learning and memory on days 50 to 53. During the training trials, STZ group animals spent a longer time finding the hidden escape box compared with animals in control or vehicle group. In contrast, the escape latency was significantly decreased in SW + STZ group compared to STZ group with no exercise (Fig. 2A (a, b)). During the probe trial, STZ group animals spent less time in the target quadrant where the escape box was formerly located, which suggests that STZ administration induced learning and memory deficits compared with normal control animals (Fig. 2A (c, d)). Interestingly, this deficit was prevented in the swim + STZ rats, indicating that exercise training before STZ injection significantly ameliorated spatial learning and memory deficits. As shown in Fig. 2B, notable deficits in recognition memory were observed in STZ-injected rats compared with control animals, as indicated by a markedly decreased preference to explore the novel object. This novel object preference was significantly elevated in swim + STZ animals, demonstrating the effectiveness of

exercise training in improving recognition memory. Of note, when we compared normal animals (no STZ injection) and normal animals with swimming exercise pretreatment, we did not find significant differences between the two groups in any of the behavioral tests mentioned above. This suggests that 4 weeks swimming pretreatment did not augment learning and memory in normal animals.

Exercise Pretreatment Significantly Inhibits STZ-induced Downregulation of Synaptic Proteins

Loss of synaptic proteins in the AD brain has been well established (16). To assess the effects of swimming exercise pretreatment on STZ-induced alteration of synaptic proteins, we next explored the expressions of synaptophysin (a presynaptic marker) and spinophilin (a postsynaptic marker) and quantified the granule density in hippocampal CA1 region. As shown in Fig. 3A, confocal imaging was taken in the stratum radiatum layer of the hippocampal CA1, and expressions of synaptophysin (red) and spinophilin (green) were decreased in STZ-injected group (Fig. 3B) as compared to control or vehicle group. Swimming exercise pretreatment was able to prevent this synaptic degradation, presenting significantly higher synaptic markers than STZ animals. Quantification analysis of the expressions of the two synaptic granules were subsequently performed, confirming these results which clearly suggests that swimming exercise pretreatment could significantly inhibit STZ-induced downregulation of synaptic protein (Fig. 3C).

Exercise Training Significantly Prevents STZ-induced Gliosis, Release of Pro-inflammatory Cytokine and Enhances the Production of Anti-inflammatory Cytokines

Neuroinflammation has been observed as a typical pathological feature of AD in both animal models and human patients, characterized by glial activation and a shift towards pro-inflammatory cytokine release over that of anti-inflammatory cytokines (1). To investigate the effect of exercise pretreatment on glial activation in the STZ AD model, immunostaining analyses of Iba-1 (a marker for microglia activation) and GFAP (a marker for reactive astrocytosis) were performed. As shown in the Fig. 4A, while the STZ animals without exercise exhibited significantly increased immunoactivity of Iba-1 (green) and GFAP (red) in hippocampal CA1 region compared to control and SW + Veh groups, SW+STZ animals had significantly less glial activation than STZ rats. In addition, we examined the effect of swimming exercise pre-training on balance of pro-inflammatory and anti-inflammatory cytokine release in the hippocampal CA1 region. As shown in Fig. 4B (a-d), results from representative confocal microscopy images of IL-10, showing remarkable decreases in the level of hippocampal IL-10 in the STZ group, as compared to control. In contrast, exercise pre-training significantly increased the expression of IL-10 and results from ELISA assays in Fig. 4B (e, f) further confirmed these shifts in IL-10 and IL-4. In addition, results from ELISA assays demonstrated that the rats with only STZ injection displayed significant increases, compared to control and SW + STZ groups, in the levels of pro-inflammatory cytokines including TNF- α , IL-1 β , IL-6 and IL-18 (Fig. 4C). Therefore, in line with the results of anti-inflammatory cytokines, exercise could significantly attenuate this pro-inflammatory response.

Exercise Pre-training Inhibits STZ-Induced Oxidative Stress and Enhances Total Antioxidant Capacity

In addition to neuroinflammation, there is increasing evidence that oxidative stress plays a critical role in the early pathology of AD (17). Therefore, we tested total antioxidant capacity, and the presence of protein carbonyls and malondialdehyde (MDA) in the hippocampal CA1 which represent the level of protein and lipid oxidation, respectively. As shown in Fig. 5A, the results of representative confocal microscopy images (a-d, red signal) and quantitative analysis (e) demonstrated that STZ induced a significant elevation of the expression of MDA compared with control group, and this increase was effectively attenuated by exercise pre-training. In addition, as shown in Fig. 5A (f), we found that STZ induced a remarkable increase of protein carbonyls, an effect that could be prevented by exercise pretreatment. Finally, the total antioxidant capacity of the SW + STZ animals, measured via an antioxidant assay kit, was also significantly increased as compared to the STZ group with no pre-training.

Exercise Pretreatment Activates Nrf2/ARE Signal Transduction Pathway and Improves the Expressions of Antioxidant Enzymes

It is known that activation of Nrf2 and its effects on downstream antioxidant gene expression confer resistance to oxidative stress in neurodegenerative diseases by modulating expression of cellular antioxidants (18, 19). Therefore, we next tested the expression and DNA-binding activity of Nrf2, as well as the expression of antioxidant enzymes including heme oxygenase 1 (HO-1), superoxide dismutase 2 (SOD2), thioredoxin 2 (TRX2), and NAD(P)H dehydrogenase [quinone] (NQO1). As illustrated in Fig. 5B, representative confocal microscopy images (a-d, red signal) and quantitative analysis (e) demonstrated a robust decrease in immunoreactivity for Nrf2 in STZ-treated animals compared to control, and a dramatic increase in SW+STZ group animals compared to STZ group with no exercise. In addition, Nrf2 DNA-binding activity was significantly impaired by STZ treatment, as shown in Fig. 5B (f), an effect which was significantly reversed by swimming pretreatment. Fig. 5C presents representative overview images of HO-1 (a-d, green), SOD2 (e-h, green), TRX2 (i-l, red) and NQO1 (m-p, red) immunoreactivity, showing an STZ-induced decrease in the presence of these Nrf2 downstream proteins which was remarkably prevented by swimming exercise pretreatment. Western blot analysis, as shown in Fig. 5C (q, r), further confirmed this effect on the expression of HO-1 and SOD2.

Exercise Pretreatment Attenuates STZ-induced A β Production and Tau Hyperphosphorylation in the Hippocampal CA1 Region of STZ-injected Rats

A β and hyperphosphorylated tau (PHF1) are key hallmarks of AD and play an important role in AD pathology. Therefore, we next investigated the effect of exercise pretreatment on the levels of A β generation and PHF1 in the hippocampal CA1. First, the immunoreactivity of A β and PHF1 protein in response to STZ injection was examined by immunofluorescence staining. As shown in Fig. 6A (a-h), STZ induced a remarkable elevation of A β (a-d, green) and PHF1 (e-h, red) signal that was inhibited by exercise pre-training. A β (1–42) levels were then determined in hippocampal protein samples using an ELISA Kit. Fig. 6A (i) indicated that STZ-induced A β generation was significantly attenuated in the SW+STZ

group. Subsequently, Western blot analysis was performed to further confirm hippocampal tau hyperphosphorylation. As shown in Fig. 6A (j), the PHF1 level was significantly elevated in STZ animals, as compared to control, which was significantly ameliorated with exercise pre-training. These effects on the classical hallmarks of clinical AD bode well for swimming pretreatment as a promising therapeutic strategy to prevent the progression of the disorder.

Exercise Pretreatment Significantly Protects Hippocampal CA1 Neurons Following STZ Injection

To examine the effect of swimming pretreatment on the survival of neurons in the CA1 region, cresyl violet staining was employed. As shown in Fig. 6B, representative microscopy images (a–d) and quantitative analysis (k) demonstrated a significant loss of surviving neurons in STZ-injected animals compared to control animals, while exercise pre-training significantly inhibited this effect. To confirm these results, TUNEL staining was performed as well. Results from confocal microscopy images (Fig. 6B (e–h)) and quantitative analysis (Fig. 6B (n)) exhibited significant apoptosis-like cell death in the STZ group in comparison with control animals, as evidenced by elevated level of TUNEL positive cells. In contrast, exercise pre-training significantly protected against this neuronal apoptosis. We also investigated the level of PARP1, as studies have indicated that overexpression of PARP1 could result in the depletion of energy and necrosis as a response to high levels of DNA damage (20, 21). As shown in Fig. 6B (i–l), STZ group presented a higher level of PARP1 immunofluorescence signal, compared to control group. The induced PARP1 expression was markedly reduced by swimming pretreatment, suggesting that physical exercise could significantly inhibit PARP1-mediated cell death.

Discussion

A β accumulation and SP are believed to be the typical pathophysiology of AD and the main culprit behind development of secondary features such as neuroinflammation, gliosis, oxidative stress, synaptic dysfunction, and neuronal apoptosis in the AD brain (1, 14). Although the exact underlying mechanisms of AD pathogenesis still remain unclear, substantial effort is under way to find effective treatments to manage or treat the disorder, one method of which is exercise training (1). In this study, we used the STZ-induced sporadic Alzheimer's rat model, a model widely accepted due to its recapitulation of several AD pathological features and behavioral phenotypes. Using this model, the present study demonstrated that exercise pretreatment was able to prevent STZ-induced pathological features of AD, presenting an amelioration of cognitive deficits regularly observed in AD patients, a marked diminution of neuroinflammation and oxidative stress, a reduction of A β production and Tau hyperphosphorylation, as well as a robust suppression of neuronal loss.

Our current study demonstrates that swimming exercise pre-training could prevent STZ-induced cognitive deficits including spatial learning and memory function in tandem with profound protection against synaptic loss. It has been established that synaptic loss, a widely characterized feature in AD, is a major correlate of cognitive impairment(14). Previous studies have further reinforced that loss of synaptic markers plays an important role in

cognitive decline in AD, even being described as the best hallmark matching the state of behavioral deterioration (22). Synaptophysin is a pre-synaptic marker which has been reported to have decreased immunoreactivity in NFT-containing neurons, suggesting the close relationship between AD cytopathology and synaptic loss (22). Although the relationship between post-synaptic markers and AD has been comparatively less studied, spinophilin, a postsynaptic marker, is substantially enriched in heads of dendritic spines and sparsely situated in other dendritic locations, and can be used as an excellent marker of dendritic spine loss (15). The current study found swimming exercise pre-training prevented the loss of both presynaptic and postsynaptic markers seen in the STZ group animals, indicating that swimming exercise pre-training confers protection to against downregulation of synaptic proteins. This profound synaptic protection was directly reflected by the prevention of spatial and object learning and memory degradation, as demonstrated in the Barnes maze and the novel object recognition test.

It is well-established that neuroinflammation plays a significant role in AD (11). In the central nervous system, astrocytes and microglial cells are often activated in neurodegenerative diseases. This glial activation is concomitant with an inflammatory response that is characterized with differential release of inflammatory cytokines (23). There are two main classes of inflammatory cytokines, pro-inflammatory and anti-inflammatory. The pro-inflammatory cytokines studied in the present study include TNF- α , IL-1 β , IL-6, IL-18 while the anti-inflammatory cytokines include IL-4 and IL-10. It has been shown that in the hippocampus of aged rats, the release of pro-inflammatory factors was enhanced and the release of anti-inflammatory factors was inhibited (24). Study has reported that the changes in this balance between pro-inflammatory and anti-inflammatory may play an important role in the pathological processes of neurodegenerative disease (25). Intriguingly, we found swimming exercise pretreatment conferred similar benefits to our previous study using treadmill exercise post-training, promoted a shift towards anti-inflammatory release and suppression of reactive gliosis (1).

Oxidative stress is a typical pathological feature of AD and has been widely accepted to play a critical role in the degenerative neuronal death (17). Normally, reactive oxygen species (ROS) are produced as by-products in the process of oxidative metabolism. During the course of aging or pathological events, oxidative burden increases due to disruptions in oxidant-antioxidant balance (26). ROS-induced damage to biomolecules, such as lipids, proteins, DNA and RNA has been proposed as a major cause in the advancement of aging and age-related neurodegenerative diseases (1). Nrf2 is a key molecule regulating the cellular antioxidant ability (27). In basal conditions, Nrf2 is bound to kelch-like ECH-associated protein 1 (Keap1) and remains in inactivation status. Once activated, Nrf2 can translocate from the cytoplasm into the nucleus and bind to ARE to active the expressions of downstream antioxidant enzymes (27). Expressions of antioxidant enzymes, such as NAD(P)H quinone oxidoreductase 1 (NQO1), are mediated by ARE play a critical role in protecting against oxidative stress. Previous studies have shown that overexpression of Nrf2 cDNA upregulated the expression of NQO1 as an response to oxidative stress, and study demonstrated mice lacking the expression of Nrf2 presented significantly decreases in the expression of NQO1 and the ability to protect the cells against redox cycling and oxidative stress (18, 19). In addition to NQO1, heme oxygenase 1 (HO-1) is another enzyme mediated

by ARE in response to oxidative stress (28). In AD, the immunoreactivity of HO-1 is significantly decreased in neurons compared with nondemented controls (9). Study found the increased expression of HO-1 can confer cytoprotection by promoting the breakdown of pro-oxidant heme to the radical scavenging bile pigments, biliverdin and bilirubin (29). TRX2 has been reported as a mitochondria-specific and a critical regulator of redox balance (30). Deletion of TRX2 induced massive apoptosis and oxidative stress, and in postmortem tissue from patients with AD, the expression of mitochondrial TRX2 was decreased, indicating the important role of Nrf2 in protection against oxidative damage (31, 32). In line with the important role of antioxidant enzymes in AD, the present study indicated that exercise pre-training exerts beneficial effects by restoring the antioxidant capacity of the AD brain, at least in part, due to the preservation of Nrf2/ARE signaling pathway and improvement of expressions of antioxidant enzymes.

The beneficial effects of exercise training on the brain have been well documented. In the brains of normal animals, physical exercise can increase the volume of the cortex and hippocampus, augment the vascular density of the brain, and can alter cerebral blood flow (33, 34). In disease states, exercise post-treatment, exercise initiating after the development of a pathological state, can ameliorate the pathogenesis of major depressive disorder (MDD), decrease the accumulation of A β , ameliorate cognitive deficits in AD and alleviate the loss of neurons and fibers in Parkinson's disease (PD) (3, 35, 36). In addition, studies found swimming could attenuate D-galactose-induced brain aging and enhance mitochondrial function and dynamics in the brain (37, 38). In addition to post-exercise, increasing numbers of studies have focused on investigating the beneficial effect of exercise preceding pathology or physiological processes. For instance, exercise pretreatment could ameliorate myocardial damage induced by prolonged intensive exercise in rats (39), and Chen et al. found that exercise pre-training for 3 weeks can improve the status of heat-stroke-induced cerebral ischemia, improving heat tolerance of animals by inducing the overexpression of heat-shock protein 72 (HSP72) (40).

The functional improvement and neuroprotective effect of exercise pre-training, in the STZ-induced sporadic AD model of the present study, was accompanied by a robust pre/post-synaptic protection, a suppression of gliosis and neuroinflammation, as well as oxidative stress, an effect likely mediate by promotion of the Nrf2/ARE pathway. Furthermore, we found that swimming exercise pre-training could decrease A β production and tau hyperphosphorylation, classical hallmarks of AD. Although further in-depth mechanistic studies about the exercise pre-training neuroprotection are still needed, the results of our study provided evidence about exercise's preventive effect against neurodegeneration and clarified contributing pathways. It is our hope that these results, along with the future work of our group and others, can lead to preventative exercise therapy that can alleviate the burden of AD in a quickly aging population.

Acknowledgments

This study was supported by Research Grant NS086929 from the National Institute of Neurological Disorders and Stroke, National Institutes of Health, USA; an American Heart Association Grant-in-Aid 15GRNT25240004, and National Natural Science Foundation grants of China: 61575065 & 11604104. The authors declare that there is no conflict of interest in the current study. The results of the study are presented clearly, honestly, and without

fabrication, or inappropriate data manipulation. The results of the present study do not constitute endorsement by ACSM.

References

1. Lu Y, Dong Y, Tucker D, et al. Treadmill Exercise Exerts Neuroprotection and Regulates Microglial Polarization and Oxidative Stress in a Streptozotocin-Induced Rat Model of Sporadic Alzheimer's Disease. *Journal of Alzheimer's disease : JAD*. 2017; 56(4):1469–84. [PubMed: 28157094]
2. Koo JH, Kang EB, Oh YS, Yang DS, Cho JY. Treadmill exercise decreases amyloid-beta burden possibly via activation of SIRT-1 signaling in a mouse model of Alzheimer's disease. *Experimental neurology*. 2017; 288:142–52. [PubMed: 27889467]
3. Nigam SM, Xu S, Kritikou JS, Marosi K, Brodin L, Mattson MP. Exercise and BDNF reduce Aβeta production by enhancing alpha-secretase processing of APP. *Journal of neurochemistry*. 2017; 142(2):286–96. [PubMed: 28382744]
4. Tapia-Rojas C, Aranguiz F, Varela-Nallar L, Inestrosa NC. Voluntary Running Attenuates Memory Loss, Decreases Neuropathological Changes and Induces Neurogenesis in a Mouse Model of Alzheimer's Disease. *Brain Pathol*. 2016; 26(1):62–74. [PubMed: 25763997]
5. Ohia-Nwoko O, Montazari S, Lau YS, Eriksen JL. Long-term treadmill exercise attenuates tau pathology in P301S tau transgenic mice. *Molecular neurodegeneration*. 2014; 9:54. [PubMed: 25432085]
6. Belarbi K, Burnouf S, Fernandez-Gomez FJ, et al. Beneficial effects of exercise in a transgenic mouse model of Alzheimer's disease-like Tau pathology. *Neurobiology of disease*. 2011; 43(2): 486–94. [PubMed: 21569847]
7. Gratuze M, Julien J, Morin F, Marette A, Planel E. Differential effects of voluntary treadmill exercise and caloric restriction on tau pathogenesis in a mouse model of Alzheimer's disease-like tau pathology fed with Western diet. *Progress in neuro-psychopharmacology & biological psychiatry*. 2017; 79(Pt B):452–61. [PubMed: 28779908]
8. McManus RM, Heneka MT. Role of neuroinflammation in neurodegeneration: new insights. *Alzheimer's research & therapy*. 2017; 9(1):14.
9. Schipper HM. Heme oxygenase expression in human central nervous system disorders. *Free radical biology & medicine*. 2004; 37(12):1995–2011. [PubMed: 15544918]
10. Wilkins HM, Carl SM, Weber SG, et al. Mitochondrial lysates induce inflammation and Alzheimer's disease-relevant changes in microglial and neuronal cells. *Journal of Alzheimer's disease : JAD*. 2015; 45(1):305–18. [PubMed: 25537010]
11. Bronzuoli MR, Iacomino A, Steardo L, Scuderi C. Targeting neuroinflammation in Alzheimer's disease. *Journal of inflammation research*. 2016; 9:199–208. [PubMed: 27843334]
12. Perry VH, Teeling J. Microglia and macrophages of the central nervous system: the contribution of microglia priming and systemic inflammation to chronic neurodegeneration. *Seminars in immunopathology*. 2013; 35(5):601–12. [PubMed: 23732506]
13. Scheff SW, Neltner JH, Nelson PT. Is synaptic loss a unique hallmark of Alzheimer's disease? *Biochemical pharmacology*. 2014; 88(4):517–28. [PubMed: 24412275]
14. Terry RD, Masliah E, Salmon DP, et al. Physical basis of cognitive alterations in Alzheimer's disease: synapse loss is the major correlate of cognitive impairment. *Annals of neurology*. 1991; 30(4):572–80. [PubMed: 1789684]
15. Akram A, Christoffel D, Rocher AB, et al. Stereologic estimates of total spinophilin-immunoreactive spine number in area 9 and the CA1 field: relationship with the progression of Alzheimer's disease. *Neurobiology of aging*. 2008; 29(9):1296–307. [PubMed: 17420070]
16. Honer WG. Pathology of presynaptic proteins in Alzheimer's disease: more than simple loss of terminals. *Neurobiology of aging*. 2003; 24(8):1047–62. [PubMed: 14643376]
17. Sun GY, He Y, Chuang DY, et al. Integrating cytosolic phospholipase A(2) with oxidative/nitrosative signaling pathways in neurons: a novel therapeutic strategy for AD. *Molecular neurobiology*. 2012; 46(1):85–95. [PubMed: 22476944]

18. Itoh K, Chiba T, Takahashi S, et al. An Nrf2/small Maf heterodimer mediates the induction of phase II detoxifying enzyme genes through antioxidant response elements. *Biochemical and biophysical research communications*. 1997; 236(2):313–22. [PubMed: 9240432]
19. Kwak MK, Wakabayashi N, Greenlaw JL, Yamamoto M, Kensler TW. Antioxidants enhance mammalian proteasome expression through the Keap1-Nrf2 signaling pathway. *Molecular and cellular biology*. 2003; 23(23):8786–94. [PubMed: 14612418]
20. Ha HC, Snyder SH. Poly(ADP-ribose) polymerase is a mediator of necrotic cell death by ATP depletion. *Proceedings of the National Academy of Sciences of the United States of America*. 1999; 96(24):13978–82. [PubMed: 10570184]
21. Berger NA. Poly(ADP-ribose) in the cellular response to DNA damage. *Radiation research*. 1985; 101(1):4–15. [PubMed: 3155867]
22. Sze CI, Troncoso JC, Kawas C, Mouton P, Price DL, Martin LJ. Loss of the presynaptic vesicle protein synaptophysin in hippocampus correlates with cognitive decline in Alzheimer disease. *Journal of neuropathology and experimental neurology*. 1997; 56(8):933–44. [PubMed: 9258263]
23. Calsolaro V, Edison P. Neuroinflammation in Alzheimer's disease: Current evidence and future directions. *Alzheimer's & dementia : the journal of the Alzheimer's Association*. 2016; 12(6):719–32.
24. Varnum MM, Ikezu T. The classification of microglial activation phenotypes on neurodegeneration and regeneration in Alzheimer's disease brain. *Archivum immunologiae et therapiae experimentalis*. 2012; 60(4):251–66. [PubMed: 22710659]
25. Tang Y, Le W. Differential Roles of M1 and M2 Microglia in Neurodegenerative Diseases. *Molecular neurobiology*. 2016; 53(2):1181–94. [PubMed: 25598354]
26. Essick EE, Sam F. Oxidative stress and autophagy in cardiac disease, neurological disorders, aging and cancer. *Oxidative medicine and cellular longevity*. 2010; 3(3):168–77. [PubMed: 20716941]
27. Zhang H, Liu H, Davies KJ, et al. Nrf2-regulated phase II enzymes are induced by chronic ambient nanoparticle exposure in young mice with age-related impairments. *Free radical biology & medicine*. 2012; 52(9):2038–46. [PubMed: 22401859]
28. Seo JY, Pyo E, An JP, Kim J, Sung SH, Oh WK. Andrographolide Activates Keap1/Nrf2/ARE/HO-1 Pathway in HT22 Cells and Suppresses Microglial Activation by Abeta42 through Nrf2-Related Inflammatory Response. *Mediators of inflammation*. 2017; 2017:5906189. [PubMed: 28373747]
29. Schipper HM, Song W. A heme oxygenase-1 transducer model of degenerative and developmental brain disorders. *International journal of molecular sciences*. 2015; 16(3):5400–19. [PubMed: 25761244]
30. Nakamura H. Thioredoxin and its related molecules: update 2005. *Antioxidants & redox signaling*. 2005; 7(5–6):823–8. [PubMed: 15890030]
31. Arodin L, Lamparter H, Karlsson H, et al. Alteration of thioredoxin and glutaredoxin in the progression of Alzheimer's disease. *Journal of Alzheimer's disease : JAD*. 2014; 39(4):787–97. [PubMed: 24270206]
32. Nonn L, Williams RR, Erickson RP, Powis G. The absence of mitochondrial thioredoxin 2 causes massive apoptosis, exencephaly, and early embryonic lethality in homozygous mice. *Molecular and cellular biology*. 2003; 23(3):916–22. [PubMed: 12529397]
33. Cahill LS, Bishop J, Gazdzinski LM, Dorr A, Stefanovic B, Sled JG. Altered cerebral blood flow and cerebrovascular function after voluntary exercise in adult mice. *Brain structure & function*. 2017
34. Clark PJ, Brzezinska WJ, Puchalski EK, Krone DA, Rhodes JS. Functional analysis of neurovascular adaptations to exercise in the dentate gyrus of young adult mice associated with cognitive gain. *Hippocampus*. 2009; 19(10):937–50. [PubMed: 19132736]
35. Shin MS, Kim TW, Lee JM, Ji ES, Lim BV. Treadmill exercise alleviates nigrostriatal dopaminergic loss of neurons and fibers in rotenone-induced Parkinson rats. *Journal of exercise rehabilitation*. 2017; 13(1):30–5. [PubMed: 28349030]
36. Salehi I, Hosseini SM, Haghighi M, et al. Electroconvulsive therapy and aerobic exercise training increased BDNF and ameliorated depressive symptoms in patients suffering from treatment-

- resistant major depressive disorder. *Journal of psychiatric research*. 2014; 57:117–24. [PubMed: 25073431]
37. Kou X, Li J, Liu X, et al. Swimming attenuates d-galactose-induced brain aging via suppressing miR-34a-mediated autophagy impairment and abnormal mitochondrial dynamics. *J Appl Physiol* (1985). 2017; 122(6):1462–9. [PubMed: 28302704]
38. Gusdon AM, Callio J, Distefano G, et al. Exercise increases mitochondrial complex I activity and DRP1 expression in the brains of aged mice. *Experimental gerontology*. 2017; 90:1–13. [PubMed: 28108329]
39. Hyun SH, Kim YM, Park SJ. The effects of preceding exercise on myocardial damage in rats. *Journal of physical therapy science*. 2017; 29(3):508–10. [PubMed: 28356642]
40. Chen YW, Chen SH, Chou W, Lo YM, Hung CH, Lin MT. Exercise pretraining protects against cerebral ischaemia induced by heat stroke in rats. *British journal of sports medicine*. 2007; 41(9): 597–602. [PubMed: 17496074]

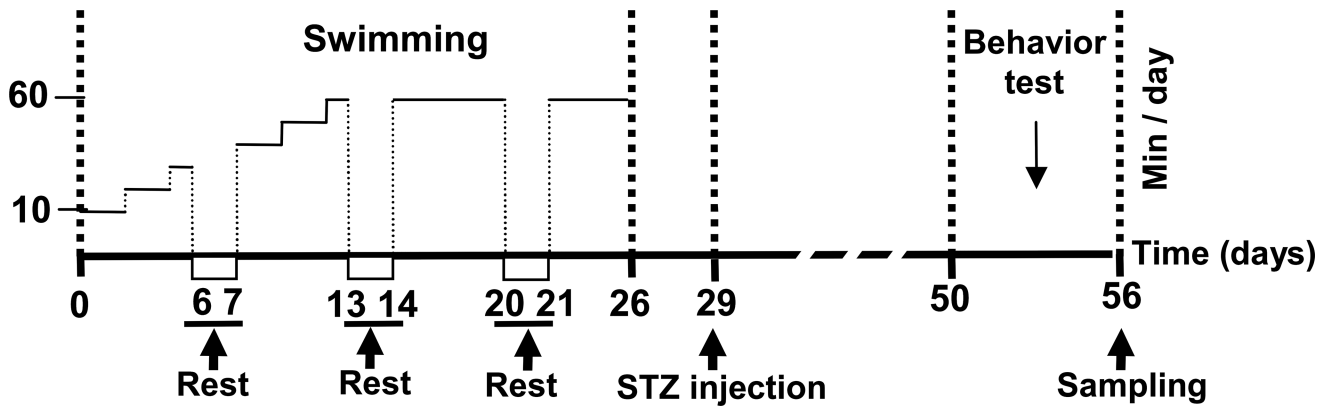


Figure 1.

Diagrammatic sketch of experimental protocol schedule. For swimming exercise pretreatment plus vehicle injection (SW + Veh) and STZ-injection group (SW + STZ), swimming exercise training was performed for 4 weeks before STZ injection. Treatment was performed 5 days/week. In the first two days, the training began with 10 min/day, and was increased by 10 min every two days until duration reached 1 h/day, occurring at day 12. After this point, training was maintained at 1 h/day until day 26. Vehicle and STZ injection was performed on day 29, and behavior tests were performed, initiating 3 weeks later. Rats were then sacrificed on day 56 and brains were collected for further analysis.

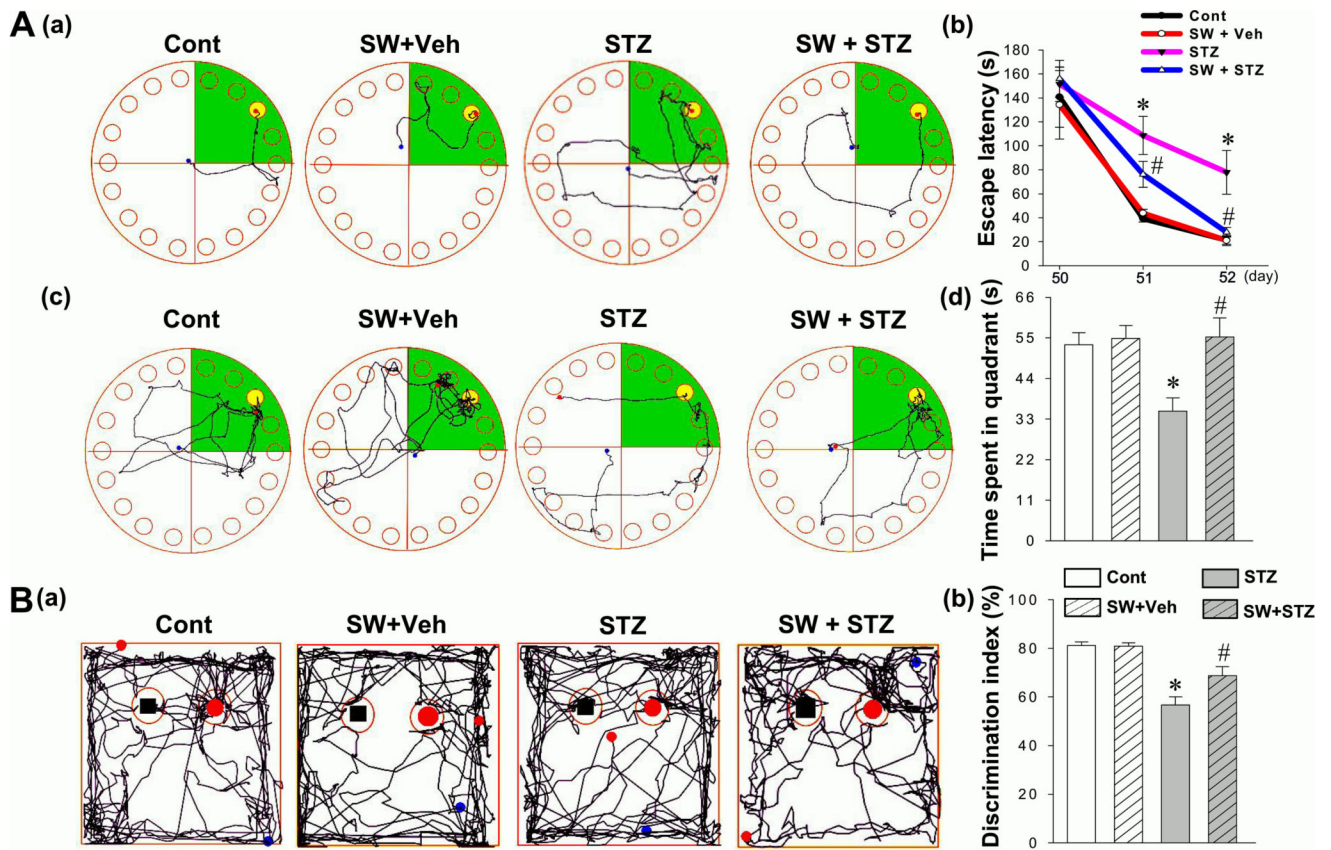


Figure 2. Effects of swimming pretreatment on STZ-induced cognitive dysfunction in rats. **(A)** The Barnes maze task was performed to test spatial learning and memory. **(a)** Representative tracking plots for control, SW + Veh, STZ and SW + STZ groups on the last training day. The escape latencies to find the black hidden box, on day 50, 51 and 52, are analyzed and shown in **(b)**. **(c)** Time spent in target quadrant (green color) on the probe trial day wherein the escape box was statistically analyzed. **(B)** Novel object recognition tests were performed to test recognition memory. **(a)** Representative traces in the choice session depicting novel object exploration are displayed. **(b)** Discrimination index was calculated and statistically compared between all groups. Data are expressed as mean \pm SE ($n = 8-10$). * $P < 0.05$ versus control group, # $P < 0.05$ versus STZ.

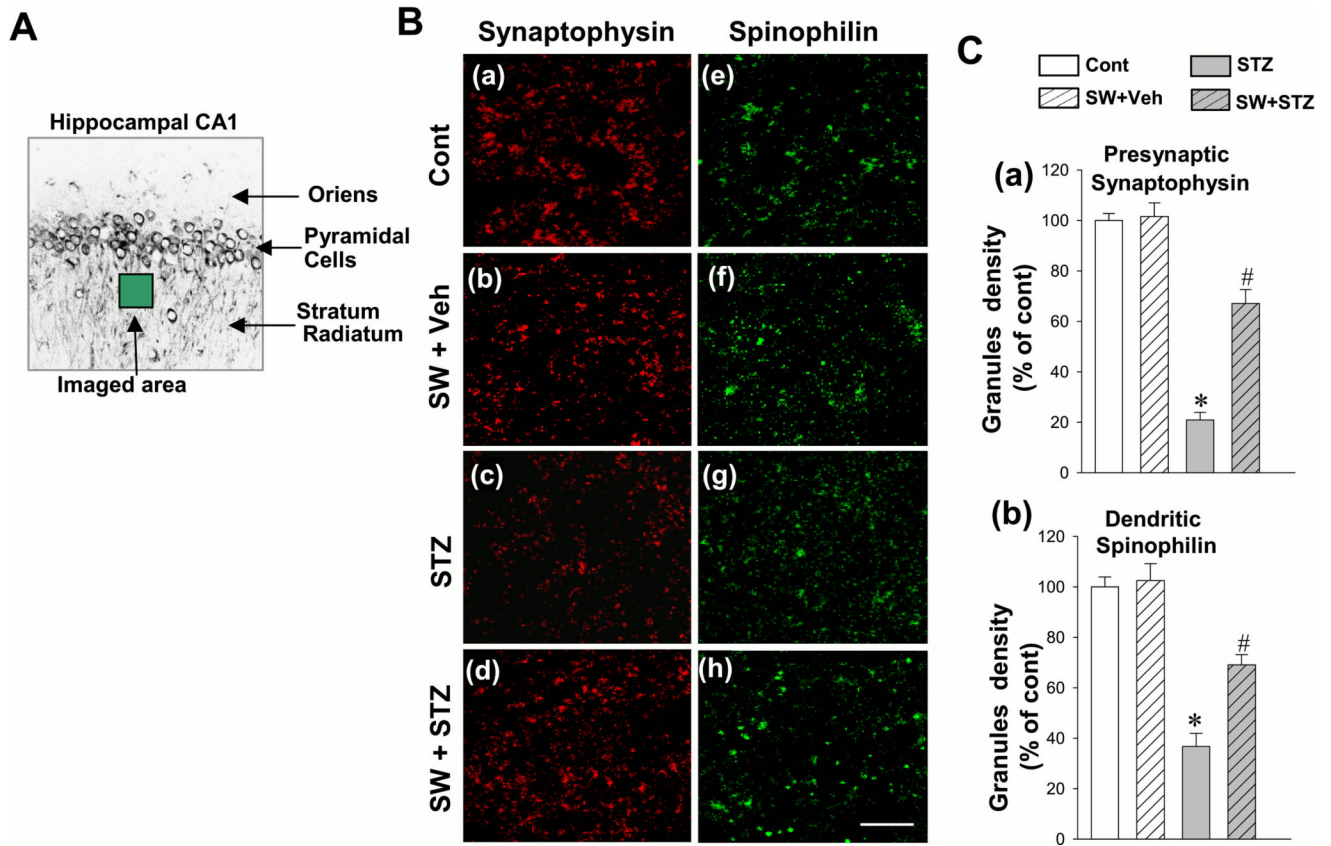


Figure 3.

Effect of exercise pretreatment on the immunoreactivity of synaptophysin and spinophilin in the rat hippocampal CA1 region. (A) The depicted area was imaged in the stratum radiatum layer of the hippocampal CA1. (B) Representative confocal microscopy images of synaptophysin (a-d, red, presynaptic marker) and spinophilin (e-h, green, postsynaptic marker) indicated that exercise pretreatment significantly prevented STZ-induced downregulation of synaptic proteins. (C) The granule density associated with synaptophysin and spinophilin was quantified. Data are expressed by mean \pm SE (n = 4–5). * P < 0.05 versus control group, # P < 0.05 versus STZ group without SW. Scale bar = 10 μ m

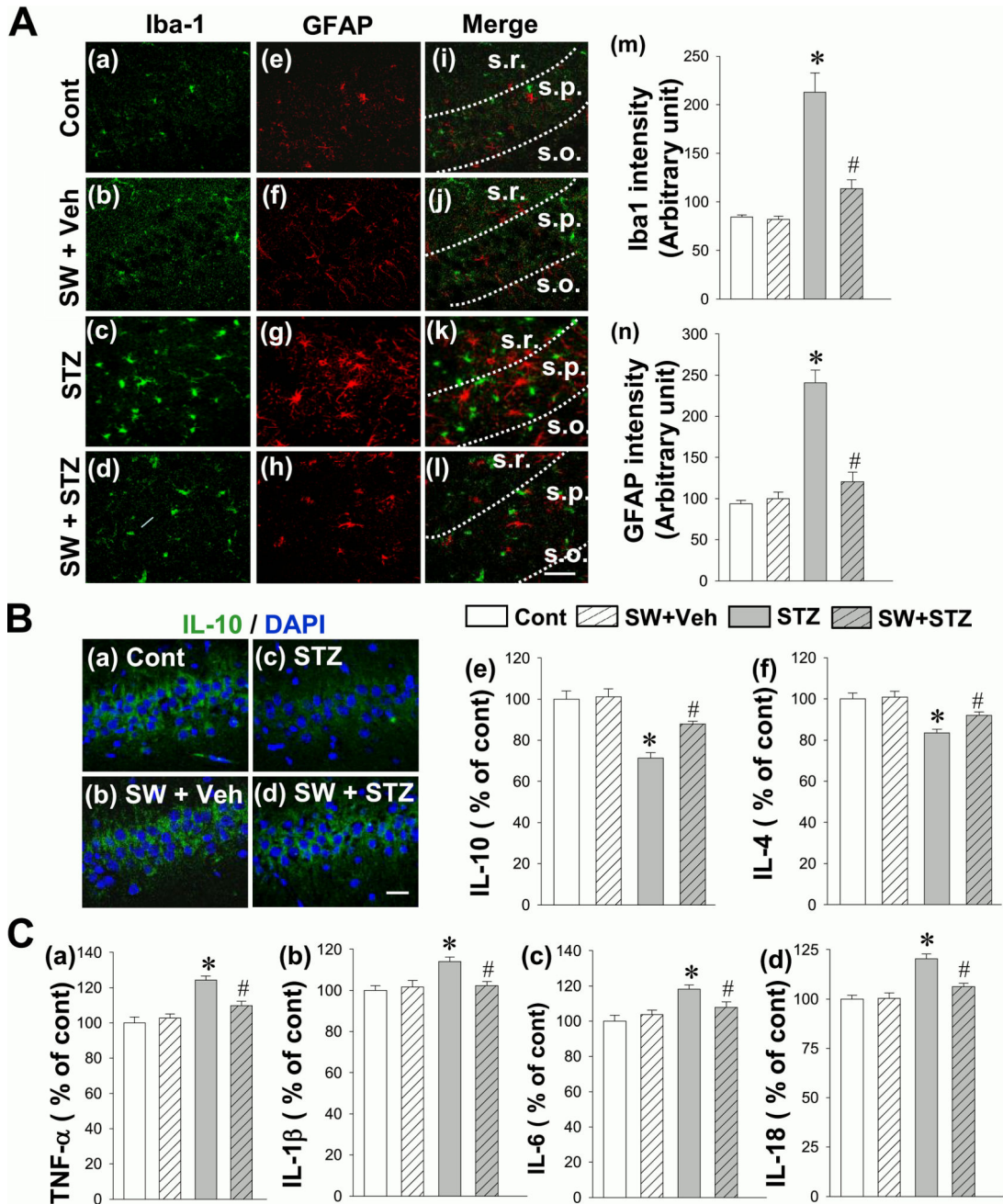


Figure 4. Effect of exercise pre-training suppresses STZ-induced gliosis, release of pro-inflammatory cytokine and enhances the production of anti-inflammatory cytokines in the rat hippocampal CA1 region. (A) Representative confocal microscopy of Iba1 (green) and GFAP (red) staining taken from medial hippocampal CA1 region (a-l). Abbreviations: s.o., stratum oriens; s.p., stratum pyramidale and s.r., stratum radiatum. The intensity of the immunoreactivity associated with Iba1 and GFAP in each group were further quantified in (m) and (n). (B). Representative confocal images of IL-10 (green) and DAPI (blue) were shown in (a-d). The levels of anti-inflammatory cytokines IL-10 and IL-4 were measured by

ELISA assay using hippocampal CA1 homogenates (e, f). (C) ELISA analyses of pro-inflammatory cytokines TNF- α , IL-1 β , IL-6 and IL-18 were performed to examine the effect of exercise pretreatment on the release of pro-inflammatory cytokines in response to STZ injection (a–d). All data are expressed as mean \pm SE (n = 4–5). * P < 0.05 versus control, # P < 0.05 versus STZ group without SW. *Scale bar* = 10 μ m.

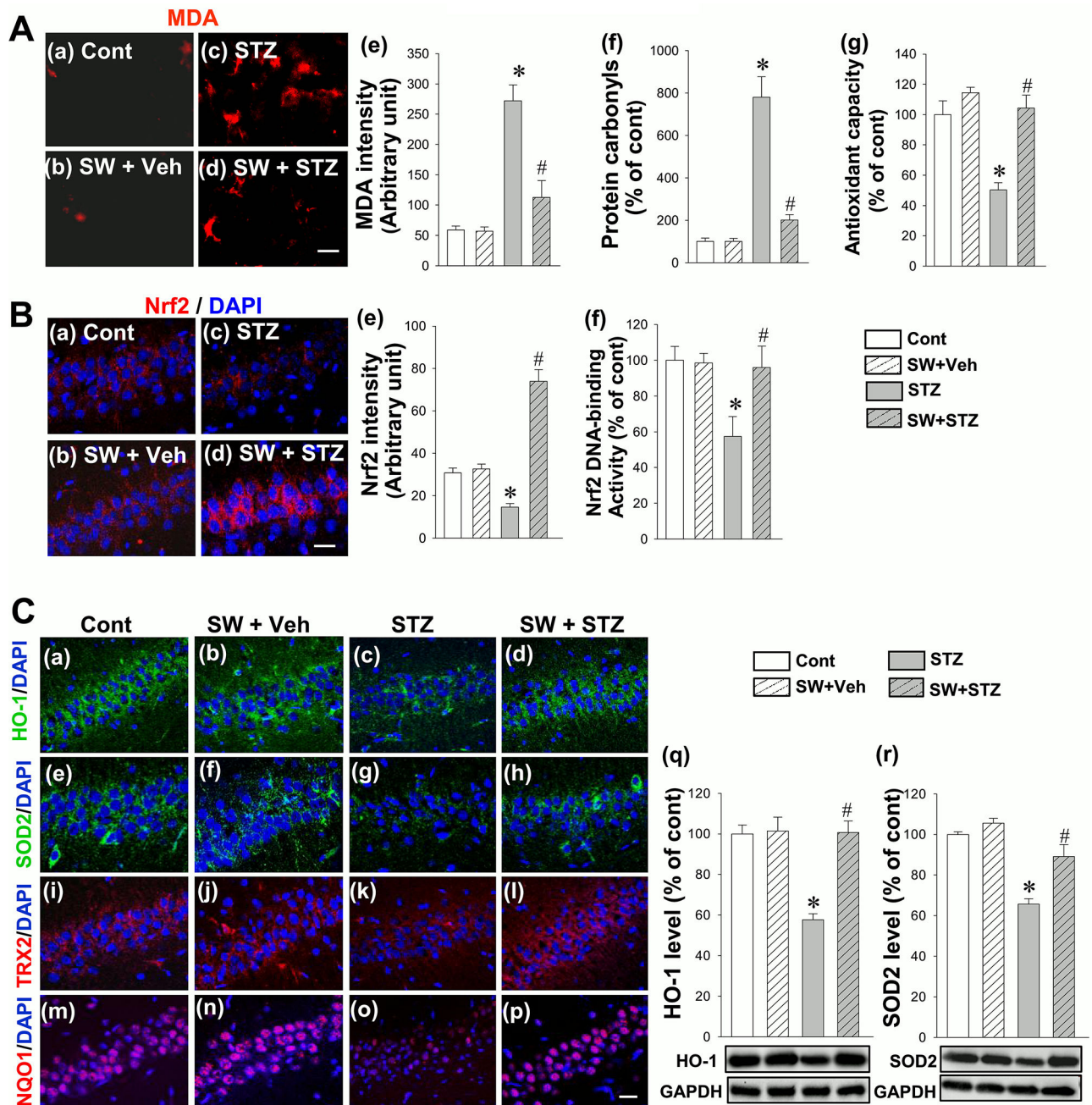


Figure 5. Effect of exercise pretreatment on STZ-induced MDA level, level of protein carbonyls, total antioxidant capacity, Nrf2 immunoactivity, Nrf2 DNA-binding activity, and the expression of HO-1, SOD2, TRX2 and NQO1 in the hippocampal CA1 region. (A) Presence of MDA was analyzed by immunofluorescence staining (a–d), and the immunoactivity associated with MDA was quantified and shown in (e). The level of protein carbonyls were measured via protein carbonyl content assay kit and shown in (f). Antioxidant assay kits were used to test the total antioxidant capacity of hippocampal CA1 homogenates (g). (B) Representative confocal images display the merged immunofluorescence signal of Nrf2 (red) and DAPI

(blue) in the medial CA1 region (a–d). The mean fluorescence signal (red) associated with Nrf2 in each group was further quantified and compared between groups (e). Nrf2 DNA-binding activity was measured and shown in (f). (C) Representative confocal microscopy images of HO-1 (a-d, green), SOD2 (e-h, green), TRX2 (i-l, red) and NQO1 (m-p, red) were shown in merged panels. Western blot analysis was performed to confirm the effect of STZ injection and exercise pretreatment on protein expression levels of HO-1 and SOD2 (q, r). All data are expressed as mean \pm SE (n = 4–5). * P < 0.05 versus control group, # P < 0.05 versus STZ group without SW. *Scale bar* = 10 μ m.

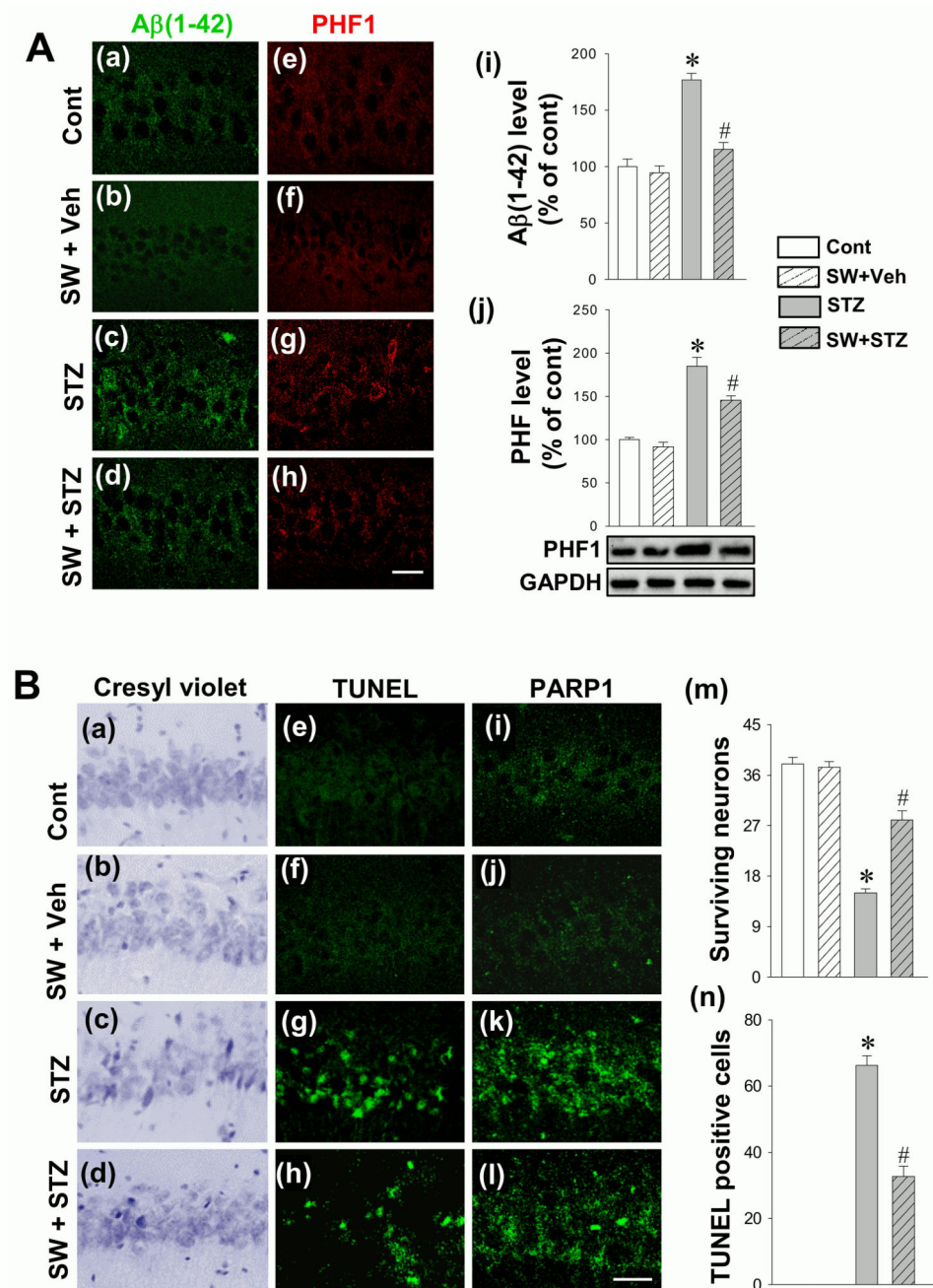


Figure 6. Effect of exercise pretreatment on STZ-induced A β accumulation, hyperphosphorylated tau (PHF1), neuronal apoptosis-like cell death and PARP1 expression in the hippocampal CA1 region. **(A)** Representative confocal images display the immunofluorescence staining of A β (a-d, green) and PHF1 (e-h, red) in hippocampal CA1 region. A β (1-42) levels were measured with an ELISA Kit using hippocampal protein samples (i). Western blot analysis was performed to further confirm the expression of PHF1 (j). **(B)** Representative images of cresyl violet staining (a-d), TUNEL staining (e-h) and PARP1 staining (i-l) in the hippocampal CA1 region are depicted. Surviving neurons (m) and TUNEL-positive cells (n)

were quantitatively analyzed. All data are expressed as mean \pm SE (n = 4–8). * $P < 0.05$ versus control group, # $P < 0.05$ versus STZ group without SW. *Scale bar* = 10 μ m.

Author Manuscript

Author Manuscript

Author Manuscript

Author Manuscript